Open Access Full Text Article

<u>*Original Research*</u>

Characterization of white matter branching in human cerebella: quantitative morphological assessment and fractal analysis of skeletonized MR images

Nataliia Maryenko[*] , Oleksandr Stepanenko

Department of Histology, Cytology and Embryology, Kharkiv National Medical University, 4, Nauky Avenue, Kharkiv, Ukraine

Correspondence

Nataliia Maryenko, Department of Histology, Cytology and Embryology, Kharkiv National Medical University, 4, Nauky Avenue, Kharkiv, Ukraine

Email: maryenko.n@gmail.com

Check for updates

BioMedPress
The Open Access Publisher

ABSTRACT

Introduction: The aim of the present study was to investigate branching characteristics of the human cerebellar white matter by the means of findings obtained from the quantitative morphological assessment and fractal analysis of the skeletonized MR images of the human cerebellum. **Methods:** Thirty individuals with no apparent brain pathology (15 males and 15 females, ranging from 18 - 30 years of age) participated in this study. Their normal T2-weighted MR images of the cerebellar vermis (midsagittal plane) were examined. The skeletonizing procedure and subsequent quantitative morphological assessment of the acquired skeletonized MR images were performed. The following parameters were determined: the number of branches, the number of junctions, the amount of end-point voxels, junction voxels and slab voxels, the average and maximum branch lengths, the longest-shortest patch length, and the number of triple and quadruple points. Additionally, the individual branches of the obtained digital skeletons of the cerebellar white matter were examined and the following parameters were assessed: branch length variability, Euclidean distance, and branch length/Euclidean distance ratio. A fractal analysis was performed using the box counting method prior to and after the MR image skeletonizing procedure. The values of the fractal dimensions (FD) of both skeletonized and non-skeletonized MR images were calculated. **Results:** It was established that the cerebella, which had the maximum values of the FD, possessed a large number of small branches approximately equal in length and which were connected by numerous junctions, forming numerous endpoints. Those cerebella, which had higher values of the average branch length and greater branch length variability, showed lower values of the FD. The key characteristics of the digital skeleton that determined the values of the FD of the cerebellum and its skeletonized MR images were the number of branches and the number of junctions that had the strongest correlational relationships with the FD of the skeletonized MR images. We submitted a proposition to consider the number of branches and amount of junctions as a diagnostic criterion in the determination of normal values of the FD. **Conclusions:** The obtained data can be used as diagnostic criteria in assessment of the morphofunctional state of the cerebellum using magnetic resonance imaging (MRI) technique.

Key words: Brain, cerebellum, fractal analysis, magnetic resonance imaging, quantitative morphological assessment, skeletonizing procedure

INTRODUCTION

Magnetic resonance imaging (MRI) technique is the most commonly neuroimaging modality used in diagnosing different organic human brain pathologies. Various morphometric tools and calculation procedures are widely employed for objective quantitative assessment of different human brain structures visualized on MR images[1–4]. The choice of the method for quantitative assessment of human brain structures presented on MR images depends on the peculiarities of their spatial configuration.

The cerebellar white matter exhibits a sophisticated tree-like branched architecture which imparts its fractal properties[5,6]. In recent years, fractal analysis has been increasingly used to assess such biological structures. The fractal dimension (FD) is a quantitative indicator of object complexity which provides a quantitative and objective estimation of the complexity degree of spatial organization and branching ratio of tree-like cerebellar structures[6–8]. There are different modifications of fractal analysis that require different software and image pre-processing algorithms[6–13].

Fractal analysis is applicable in different fields of neuroscience[6,7,14], including neuroimaging (MRI of brain and computed tomography)[15–24], computational studies of neurons[8,23–26], and fractal analysis of vascular network of brain structures[27–29].

A skeletonizing technique is one of the digital image pre-processing procedures which reveals the framework of the structure — its digital skeleton[12,30,31]. The skeletonized version of the MR image of the cerebellum corresponds to the main branches of the cerebellar white matter; it is the digital framework of the cerebellar "arbor vitae". Modern-day software programs for digital image analysis (for instance, Image J) enable the skeletonizing procedure of MR images and a subsequent quantitative morphologic assessment of the acquired digital skeletons. The quantitative analysis evaluates the main parameters of the skeletonized MR image (number of branches, number of junctions, amount of endpoint voxels and parameters of individual branches) that characterize its architecture and the degree of branching.

A combination of skeletonizing technique with quantitative analysis of the skeletonized digital images has been used to study different tree-like structures (mainly dendritic trees of neurons)[32–34]. In some research studies, the skeletonizing procedure has been carried out as a pre-processing method of the cerebellar MR images to obtain further FD analysis[12]. However, the skeletonizing procedure and quantitative analysis of digital skeletons of the cerebellar white matter have not been used before for assessment of anatomical structures on cerebellar MR images as a diagnostic algorithm.

In the present study, we implemented a combination of fractal analysis and quantitative morphological assessment of the skeletonized cerebellar MR images to quantitatively examine the branching characteristics of the human cerebellar white matter and determine the factors which specify these characteristics.

METHODS

Materials

The study was conducted in compliance with the basic bioethical provisions of the Council of Europe Convention on Human Rights and Biomedicine (March 4, 1997), the Helsinki Declaration of the World Medical Association on the ethical principles of scientific medical research with human participation (1964-2008), and the order of Ministry of Health of Ukraine No. 690 (dated Sept. 23, 2009). The conclusion of the Commission on Ethics and Bioethics of Kharkiv National Medical University confirmed that the study was conducted in compliance with human rights, in accordance with the current legislation in Ukraine, met international ethical requirements and did not violate ethical standards in science and standards of biomedical research (minutes of the meeting of the commission on ethics and bioethics of KhNMU No. 10 of Nov. 7, 2018).

In this research study, T2-weighted MR images of the cerebellar vermis (midsagittal plane) were studied obtained from 30 subjects (15 males and 15 females with age range of 18-30 years) who underwent diagnostic MRI scanning of the brain at the Radiologic Center in Kharkiv, and showed no apparent brain pathology upon examination. Their MRI data were considered as relatively normal.

MRI was performed on a 1.5 T MRI machine (Siemens Magnetom Symphony, Munich, Germany). The image parameters included the following: TE (echo time) of 122 ms, TR (repetition time) of 4520 ms, and section thickness of 5 mm.

Methods

Image pre-processing

A 2×2-inch (128×128-pixels) fragments containing the midsagittal sections of the cerebella were copied from the digital MR images. Afterwards, the fragments of MR images were pre-processed with the help of Adobe Photoshop CS5 software (Adobe Inc., California, USA) for further skeletonizing procedure and fractal analysis. During this pre-processing, the structures surrounding the cerebella were initially removed from the images (**Figure 1A**), and the pixels in these areas were colored white (brightness value of 255). Next, the segmentation of the MR images of the cerebella into two components was performed - into the studied structures (cerebellar tissue as a whole) and the background. For that purpose, we used the "threshold" tool which converted the MR images to binary format which resulted in MR image segmentation according to the pixel brightness value. An empirical brightness threshold value of 100 was used for the localization of cerebellar tissue on MR images. As a result of the pre-processing and segmentation procedures of the MR images, the pixels corresponding to the cerebellar tissue were black (brightness value of 0) and the pixels corresponding to the background were white (brightness value of 255) (**Figure 1 B**). Further processing and FD analysis of the binary images were performed with the Image J software.

Analysis of skeletonized MR images

The digital image skeletonizing procedure was performed using the "skeletonize" tool. This tool revealed the main branches of the cerebellar white matter and formed a linear digital skeleton of the white matter — the "arbor vitae" of the cerebellum (**Figure 1 C**).
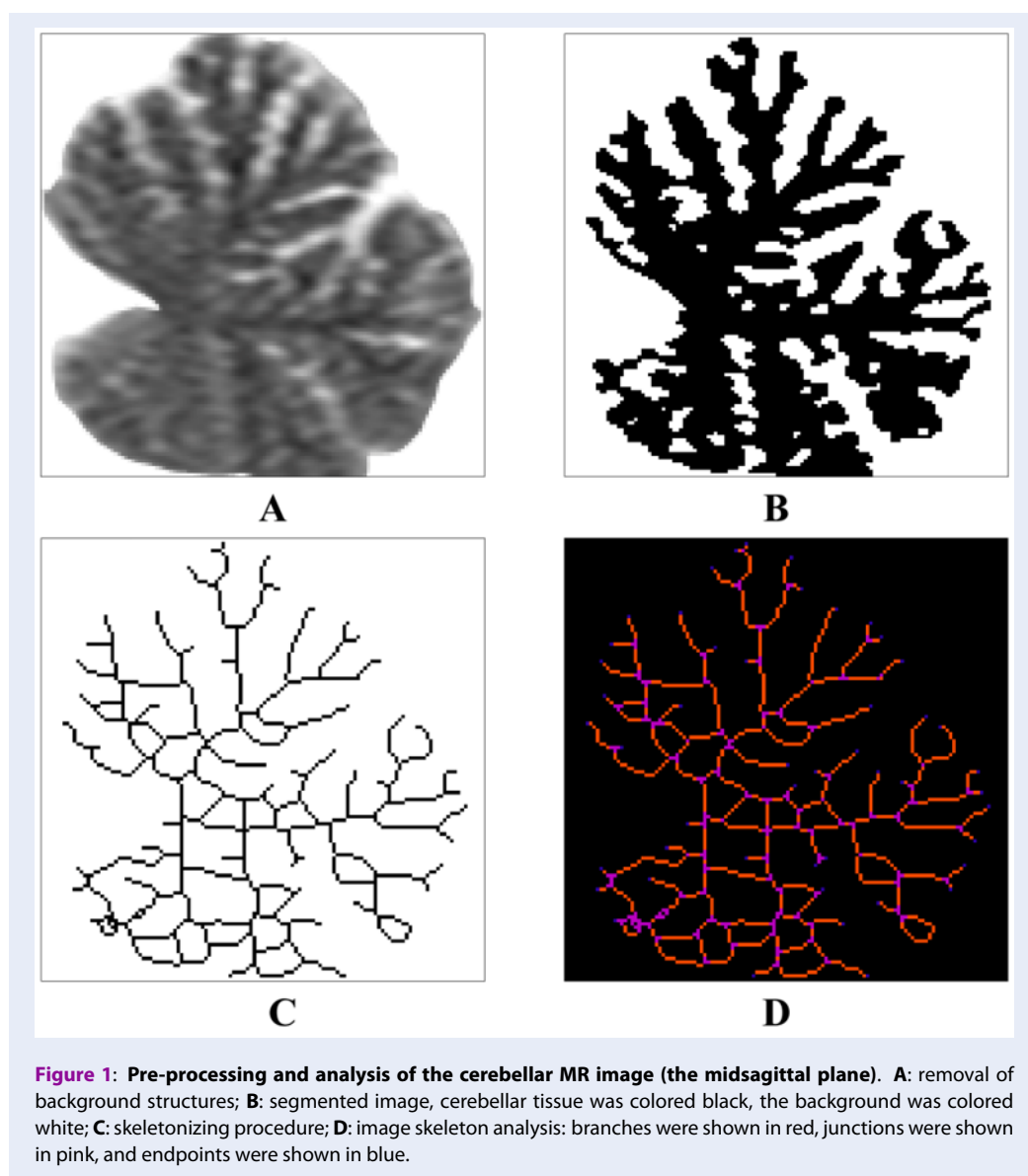
Figure 1: **Pre-processing and analysis of the cerebellar MR image (the midsagittal plane)**. **A**: removal of background structures; **B**: segmented image, cerebellar tissue was colored black, the background was colored white; **C**: skeletonizing procedure; **D**: image skeleton analysis: branches were shown in red, junctions were shown in pink, and endpoints were shown in blue.

Furthermore, the skeletonized images were analyzed using the "analyze skeleton" tool (**Figure 1 D**). The following parameters were estimated: the number of branches, the number of junctions, the amount of end-point voxels, junction voxels and slab voxels, the average and maximum branch lengths, the longest-shortest patch length, and the number of triple and quadruple points.

We also analyzed the individual branches of the digital skeletons of the cerebellar white matter. The following parameters were determined: branch length variability, Euclidean distance, and branch length/Euclidean distance ratio. In total, the morphologic parameters of 4130 branches of 30 cerebella were calculated.

Fractal analysis

The fractal analysis was carried out using the box counting method tool of the Image J software. The values of the two-dimensional FD were determined. The fractal analysis was performed twice: prior to and after the skeletonizing procedure. As a result, two FD were obtained: FD (100) — fractal dimension of non-skeletonized MR images (which characterized the cerebellar tissue as a whole), and FD (S) — fractal dimension of skeletonized MR images (which characterized the skeleton of the cerebellar white matter).

Statistical data processing

A statistical data processing was done using Excel 2010 software. The following values were calculated: the sample mean (M), the standard error of the mean (m), standard deviation (σ), coefficient of variation (CV, relative standard deviation), the minimum (min) and the maximum (max) values, the median (Me), and the mode (Mo). The distribution of the values by the percentiles was determined. The significance of the statistical differences between the values of FD(S) and FD(100) was assessed using Student's T test. The significance of statistical differences between the values of the quantitative parameters of different cerebellar clusters was assessed using the Mann-Whitney test. Pearson's correlation coefficient (R) was calculated to establish the relationships between the values. The significance of the correlation was assessed using Student's T test. The significance level for all results was accepted as $p < 0.05$.

RESULTS

Quantitative characteristics of skeletonized images of human cerebella

The values of the quantitative parameters of the cerebellar white matter are presented in **Table 1.** Most of the parameters had mean values of the coefficient of variation; the value of quadruple points had a high coefficient of variation. The mean values of these parameters and the confidence interval of the values (calculated as $M \pm 2\sigma$) may be used as norm criteria to interpret the results of the quantitative morphological assessment of the cerebellar MR skeletonized images.

Quantitative characteristics of white matter branches of human cerebella

Morphometric parameters of 4130 branches of the skeletonized MR images of the cerebellum were estimated. The mean value of the branch length was 3.85 ± 0.04 m^{-3} (min — 0.40 m^{-3}, max — 16.59 m^{-3}) (**Figure 2**). As can be seen from the data in **Figure 3,** the statistical distribution of the branch length had a right-hand asymmetry; the values of the sample mean (3.85 m^{-3}), the mode (1.92 m^{-3}) and the median (3.43 m^{-3}) did not coincide. Thus, the distribution of the values by the percentiles was determined to describe the statistical distribution. The value of the percentile 2.5 was 0.56 m^{-3}, percentile 16 – 1.75 m^{-3}, percentile 25 – 2.25 m^{-3}, percentile 50 – 3.43 m^{-3}, percentile 75 – 4.98 m^{-3}, percentile 84 – 5.86 m^{-3}, and percentile 97.5 – 9.81 m^{-3}. The mean value of the Euclidean distance of the white matter branches was 3.4 ± 0.03 m^{-3} (min — 0.40 m^{-3}, max — 15.33

m^{-3}). The mean value of the ratio of branch length and Euclidean distance was 1.13 ± 0.003 (min — 1, max — 4.16). The branch length value was very close to the value of the Euclidean distance and often coincided with it or exceeded it by 1.1 - 1.2 times, sometimes more than 4 times. There was a significantly strong positive linear relationship between the values of branch length and Euclidean distance (R = 0.97, p $\approx$ 0). The distributions of these parameters are presented in **Figure 3.**

Correlational relationships of quantitative characteristics of skeletonized MR images of human cerebella

The strength and direction of the correlation relationships between the quantitative characteristics of the skeletonized MR images of human cerebella were different. As can be seen from **Table 2,** there were significant positive linear correlational relationships between the number of branches, the number of junctions, the amount of end-point voxels, junction voxels and slab voxels, the average and maximum branch lengths, the longest-shortest patch length, and the number of triple and quadruple points. The numbers of branches, junctions, end-point voxels, junction voxels, triple points and quadruple points had significant negative linear correlation relationships with the average branch length, the branch length variability (the coefficient of variation), and the maximum branch length.

Therefore, the more branched the white matter of the cerebellum was, the more branches, junctions and end points it had. The cerebellum with a high degree of branching of the white matter had a lot of short branches and junctions. The cerebellum with less branched white matter did not have numerous branches and junctions; their length of branches was greater and more variable than in those cerebella with greater branching degree.

Clusters of cerebella according to white matter branching features

Taking into consideration features of the branching characteristics of the digital skeletons of the cerebellar white matter, we can assume that the key characteristics of its branching pattern are the number of branches and the number of junctions. These parameters (number of branches and junctions) were related by a correlation relationship close to the functional one (R = 0.99, p = 0.11×10^{-35}). It was easier to determine the number of branches than number of junctions (if manual count was used and image

Table 1: Statistical data of the quantitative morphological assessment of the skeletonized MR images of human cerebellum

| Parameter	M	m_m	M_e	σ	C_v	m_{cv}	min	max
Branches	120.03	4.70	124.50	25.73	21.44	3.056	67	168
Junctions	60.60	2.55	63.50	13.94	23.00	3.197	30	86
End-point voxels	40.83	1.50	40.00	8.24	20.18	2.759	28	58
Junction voxels	239.10	10.32	239.50	56.52	23.64	3.408	134	353
Slab voxels	734.03	25.94	747.00	142.09	19.36	2.428	405	973
Average branch length, m^{-3}	4.02	0.08	3.98	0.44	11.00	1.40	3.19	5.10
Branch length variability (CV, %)	59.31	1.21	57.14	6.62	11.16	0.662	48.89	77.54
Maximum branch length, m^{-3}	12.97	0.43	12.95	2.39	18.42	2.34	7.93	16.59
Euclidean distance m^{-3}	3.46	0.08	3.37	0.45	13.00	1.65	2.78	4.59
Branch length/Euclidean distance	1.13	0.003	1.080	0.17	14.88	0.164	1.00	4.16
Longest shortest patch m^{-3}	73.70	1.13	73.13	6.31	8.56	1.09	64.07	86.04
Triple points	46.97	1.97	50.00	10.78	22.96	3.030	19	65
Quadruple points	10.50	0.78	10.00	4.25	40.46	5.700	3	24
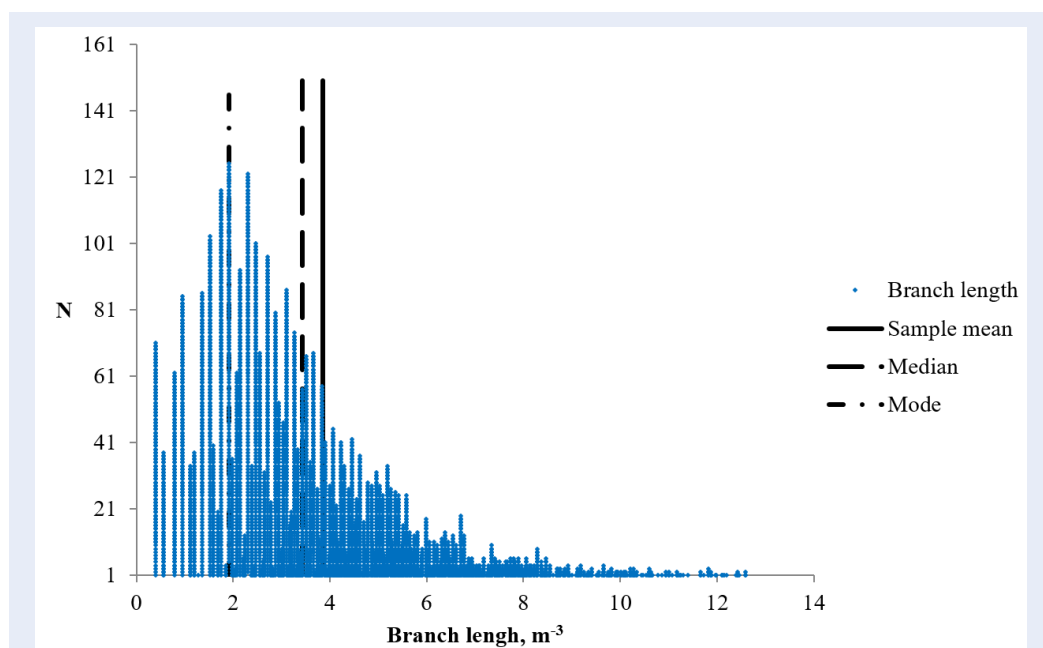
Figure 2: The length of the branches of skeletonized MR images of cerebellum and it's prevalence.
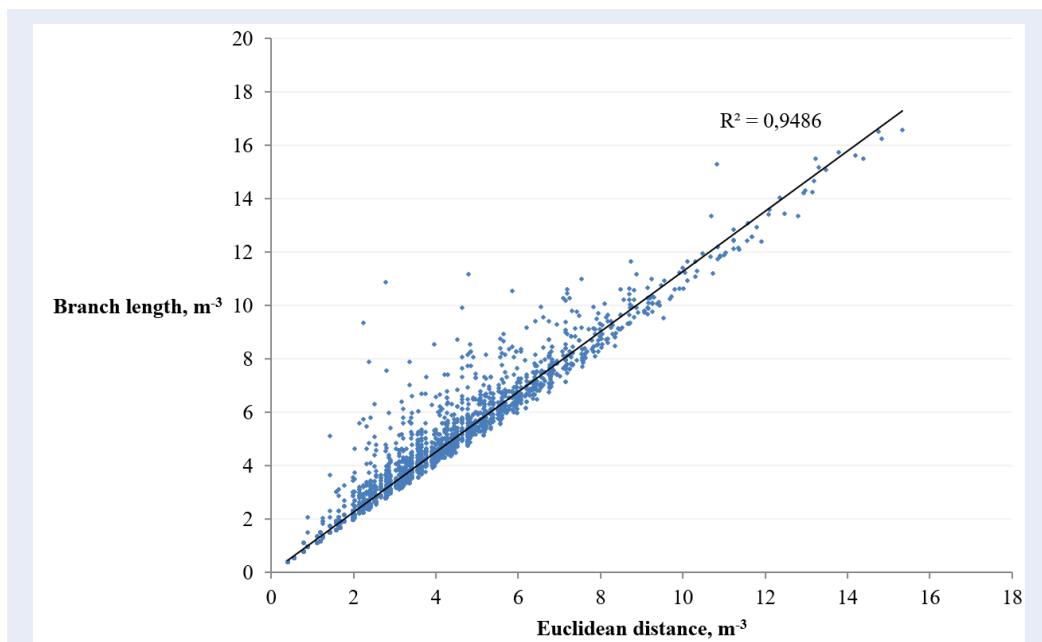
Figure 3: **Relationship between the length and Euclidean distance of the branches of skeletonized MR images of human cerebellum.**
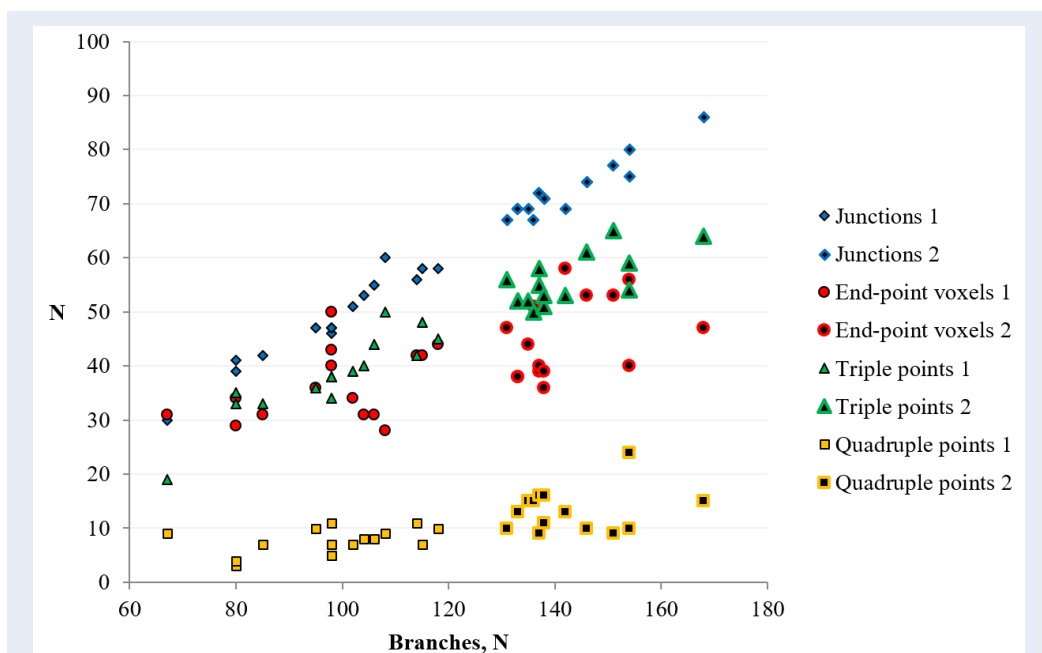

Figure 4: **Quantitative characteristics of the skeletonized images of the first (1) and the second (2) clusters of cerebella.**

Table 2: Correlation relationships between the parameters of the skeletonized MR images of human cerebellum (Pearson's correlation coefficients (R))

Parameter		1	2	3	4	5	6	7	8	9	10	11	12
1	Branches	-	0.99^3	0.72^3	0.98^3	0.71^3	-0.52^2	-0.59^3	-0.44^1	-0.32	0.49^2	0.94^3	0.77^3
2	Junctions	0.99^3	-	0.64^3	0.97^3	0.75^3	-0.48^2	-0.63^3	-0.44^1	-0.26	0.48^2	0.96^3	0.76^3
3	End-point voxels	0.72^3	0.64^3	-	0.64^3	0.34^1	-0.63^3	-0.25	-0.46^2	-0.53^2	0.38^1	0.65^3	0.43^1
4	Junction voxels	0.98^3	0.97^3	0.64^3	-	0.68^3	-0.50^2	-0.57^3	-0.40^1	-0.31	0.47^2	0.89^3	0.80^3
5	Slab voxels	0.71^3	0.75^3	0.34^1	0.68^3	-	0.18	-0.65^3	-0.06	0.36^1	0.70^3	0.72^3	0.59^3
6	Average branch length, m^{-3}	-0.52^2	-0.48^2	-0.63^3	-0.50^2	0.18	-	0.01	0.55^2	0.93^3	0.18	-0.48^2	-0.31
7	Branch length variability (CV, %)	-0.59^3	-0.63^3	-0.25	-0.57^3	-0.65^3	0.01	-	0.43^1	-0.21	-0.33	-0.65^3	-0.42^1
8	Maximum branch length, m^{-3}	-0.44^1	-0.44^1	-0.46^2	-0.40^1	-0.06	0.55^2	0.43^1	-	0.44^1	0.03	-0.50^2	-0.19
9	Euclidean distance m^{-3}	-0.32	-0.26	-0.53^2	-0.31	0.36^1	0.93^3	-0.21	0.44^1	-	0.23	-0.25	-0.19
10	Longest shortest patch m^{-3}	0.49^2	0.48^2	0.38^1	0.47^2	0.70^3	0.18	-0.33	0.03	0.23	-	0.44^1	0.40^1
11	Triple points	0.94^3	0.96^3	0.65^3	0.89^3	0.72^3	-0.48^2	-0.65^3	-0.50^2	-0.25	0.44^1	-	0.58^3
12	Quadruple points	0.77^3	0.76^3	0.43^1	0.80^3	0.59^3	-0.31	-0.42^1	-0.19	-0.19	0.40^1	0.58^3	-

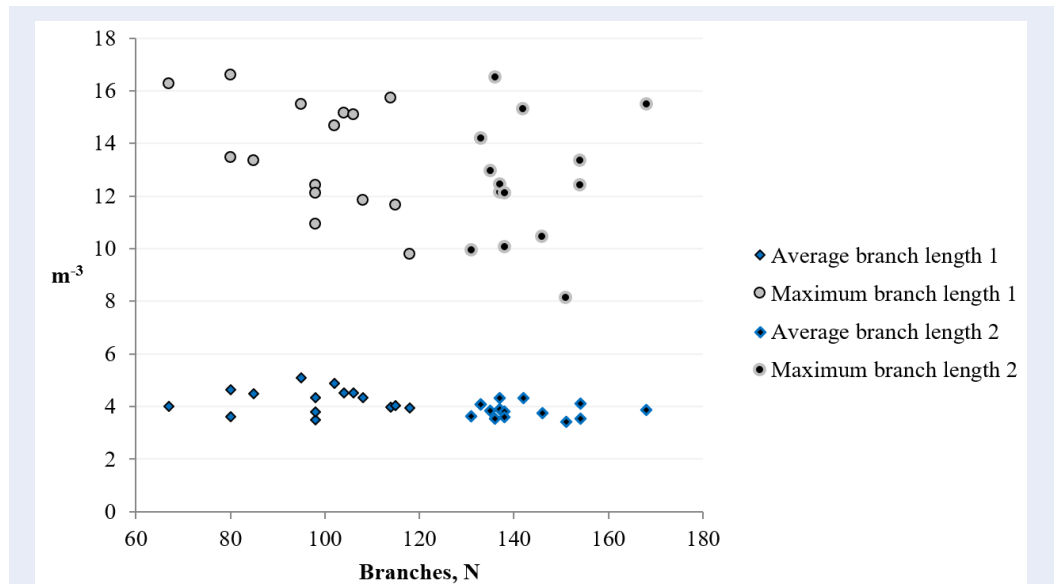*Note*: [1]: p < 0.05; [2]: p < 0.01; [3]: p < 0.001

Figure 5: **The branch lengths (average and maximum) of the cerebella of the first (1) and the second (2) clusters.**
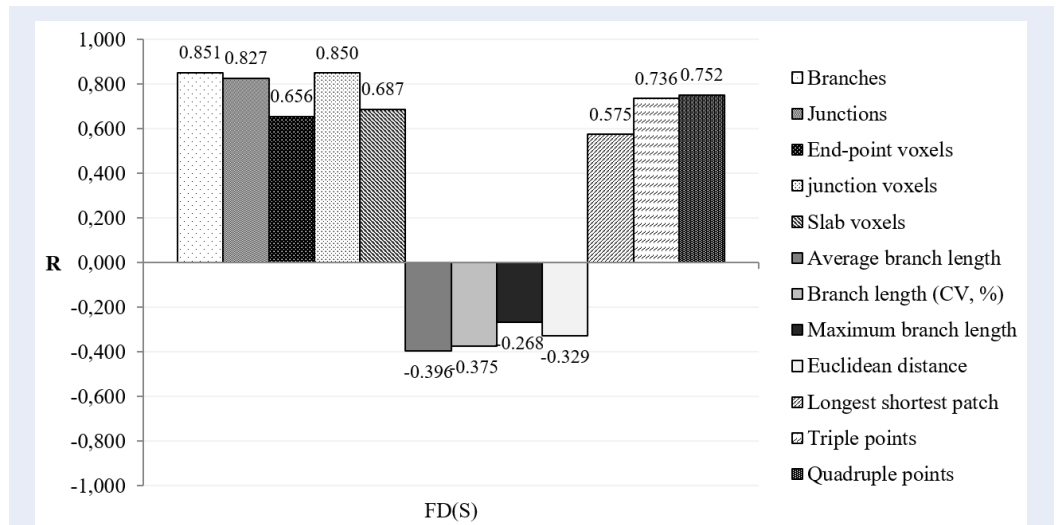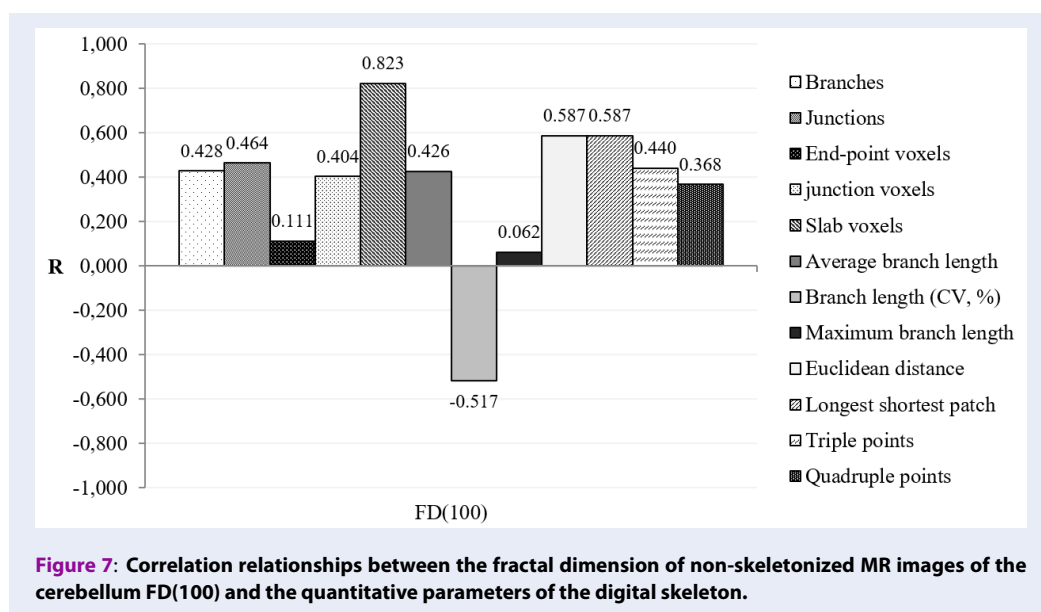

Figure 6: **Correlation relationships between the fractal dimension of skeletonized MR images of the cerebellum FD(S) and the quantitative parameters of the digital skeleton.**

skeletonizing procedure was not applied). Thus, the number of branches was chosen as a key characteristic to divide cerebella into clusters and to determine features of other quantitative parameters in different cerebellar clusters. We divided cerebella into two clusters according to the median value of the number of branches (130). The number of branches in cerebella of the first cluster was 130 or less, and the second cluster was 131 or more. These clusters had some differences in the distribution of the values of quantitative

parameters of the digital skeletons of MR images of cerebellar white matter (**Figures 4 and 5**).

The mean number of junctions in cerebella of the first cluster was 48.67 ± 2.16, and of the second cluster was 74.38 ± 2.31; the mean number of the end-point voxels was 36.40 ± 1.71 (1st cluster) and 46.38 ± 2.17 (2nd cluster); the mean number of the triple points was 38.27 ± 1.94 (1st cluster) and 56.56 ± 1.50 (2nd cluster); and the mean number of the quadruple points was 7.73 ± 0.62 (1st cluster) and 14.00 ± 1.23 (2nd

Figure 7: **Correlation relationships between the fractal dimension of non-skeletonized MR images of the cerebellum FD(100) and the quantitative parameters of the digital skeleton.**

cluster).

The mean value of the average branch length in cerebella of the first cluster was 4.24 ± 0.12 m^{-3}, of the second cluster — 3.86 ± 0.07 m^{-3}; the mean value of the maximum branch length in cerebella of the first cluster was 13.64 ± 0.54 m^{-3}, of the second cluster — 12.65 ± 0.60 m^{-3}.

The differences between the values of these parameters of the cerebella of the first and second clusters were statistically significant ($p < 0.05$).

Fractal analysis of MR skeletonized images of cerebellum

The fractal analysis was performed to evaluate the degree of complexity of the spatial organization of the cerebellar tissue as a whole and its skeletonized MR images. The mean value of FD(100) (fractal dimension of the cerebellar tissue as a whole) was 1.738 ± 0.009 (min — 1.634, max — 1.823). The coefficient of variation of FD(100) was 3.06% which indicated a low degree of variation. The average value of FD(S) (fractal dimension of skeletonized MR images) was 1.469 ± 0.007 (min — 1.360, max — 1.551). The coefficient of variation of FD(S) was 2.76%, which also showed a low degree of variation. Both values of FD were statistically significantly different from each other ($p = 0.215 \times 10^{-25}$). There was a moderate positive linear correlation relationship between FD(100) and FD(S) ($R = 0.41$, $p = 0.016$). These values of the FD had correlation relationships of different strength and direction with the quantitative parameters of the skeletonized MR images (**Figures 6 and 7**).

As can be seen from **Figure 6,** FD(S) had significant positive linear correlation relationships with the number of branches ($p = 0.143 \times 10^{-7}$), the number of junctions ($p = 0.644 \times 10^{-7}$), the number of end-point voxels ($p = 0.959 \times 10^{-4}$), the number of junction voxels ($p = 0.14 \times 10^{-7}$), the number of slab voxels ($p = 0.43 \times 10^{-4}$), the longest-shortest patch length ($p = 0.788 \times 10^{-3}$), the number of triple points ($p = 0.786 \times 10^{-5}$), and the number of quadruple points ($p = 0.413 \times 10^{-5}$). FD(S) had significant negative linear correlation relationships with the average branch length ($p = 0.019$), the branch length variability (the coefficient of variation of branch length) ($p = 0.028$), the maximum branch length ($p = 0.125$), and the Euclidean distance ($p = 0.049$).

The FD of the cerebellar tissue as a whole (FD(100)) had a similar tendency to increase or decrease depending on the quantitative parameters of the skeletonized MR images but it had weaker strength of correlation relationships with these parameters than FD(S) (**Figure 7**). As can be seen from **Figure 7**, FD(100) had significant positive linear correlation relationships with the number of branches ($p = 0.012$), the number of junctions ($p = 0.007$), the number of junction voxels ($p = 0.018$), the number of slab voxels ($p = 0.103 \times 10^{-6}$), the longest-shortest patch length ($p = 0.603 \times 10^{-3}$), the number of triple points ($p = 0.01$), and the number of quadruple points ($p = 0.031$). FD(100) had a significant negative linear correlation relationship with the coefficient of variation of branch length ($p = 0.002$). However, FD(100) had no significant correlation relationships with the

number of end-point voxels (p = 0.952) or maximum branch length (p = 0.997), and had significant positive linear correlation relationships with the average branch length (p = 0.012) and Euclidean distance (p = 0.603×10^{-3}).

The mean value of FD(S) of cerebella of the first cluster (described according to the number of branches) was 1.438 ± 0.01, of the second cluster — 1.495 ± 0.01. The difference between FD(S) values of cerebella of the first and second clusters was significant (p < 0.05). The mean FD(100) value of cerebella of the first cluster was 1.720 ± 0.01, of the second cluster — 1.753 ± 0.01; however, the difference between these values was not significant (p > 0.05).

Hence, there were two groups of quantitative parameters of digital skeletons which had an impact on the values of the FD. The first group included parameters that characterized the branching of the digital skeletons (branches, junctions, junction voxels, end-point voxels, and triple and quadruple points). They were interconnected by positive correlation relationships (inside the group), had positive correlation relationships with the fractal dimensions FD(S) & FD(100), and showed negative correlation relationships with the parameters of the second group, including the average and maximum branch length, Euclidean distance, and the coefficient of variation of branch length (branch length variability, CV). The parameters of the second group exhibited negative correlation relationships with the fractal dimensions.

The cerebella, which had the maximum values of the FD, contained a larger number of small branches approximately equal in length which were connected by numerous junctions and which formed numerous endpoints. Those cerebella that had larger values of the average branch length and greater branch length variability demonstrated lower values of the FD.

It became obvious that the key characteristics of the digital skeletons that determine the values of the FD of the cerebellum and its skeletonized MR images were the number of branches and the number of junctions that showed the strongest correlation relationships with the FD of the skeletonized MR images FD(S) (**Figure** 7). The same parameters (the number of branches and their junctions) were used for calculation of the confidence intervals of the FD values of the skeletonized MR images of the human cerebellum.

The number of branches and their junctions remain constant throughout life, as they characterize the innate anatomical features of the white matter of the cerebellum. However, the FD of the cerebellum can change during some brain diseases [10–13] and may be used as an objective morphometric criterion for the diagnosis of these pathologies. Therefore, considering the fact that the FD strongly depends on the number of branches and their junctions, which have a distinct individual variability and do not change throughout life, we propose to consider these parameters for determination of the normal value of FD as a diagnostic criterion.

DISCUSSION

In this study we aimed to determine the branching characteristics of the white matter of human cerebella through the combined use of quantitative morphological assessment and fractal analysis of the skeletonized MR images of the cerebellum. We estimated values of quantitative parameters and FD of skeletonized, as well as non-skeletonized MR images of the human cerebellum.

The main finding of the present study is that quantitative parameters of the digital skeletons of the MR images of the cerebellar white matter (*e.g.* branching characteristics) have an impact on the values of the cerebellar fractal dimensions. The conducted investigation has enabled us to subdivide the studied quantitative parameters into 2 groups according to their type of correlation relationship with the fractal dimension. The first group includes the number of branches, the number of junctions, the amount of junction and end-point voxels, and the number of triple and quadruple points. These parameters have positive correlation relationships with each other and exhibit positive correlation relationships with the fractal dimension. The second group of quantitative parameters includes the average and maximum branch lengths, the Euclidean distance, and the branch length variability. These parameters have negative correlation relationships with the parameters of the first group and with FD. Thus, the fractal dimension of skeletonized MR images of cerebellum increases concurrently with the numbers of branches, junctions, junction voxels, end-point voxels, and triple and quadruple points.

We conclude that the number of branches and the number of junctions exert the biggest impact on the fractal dimension. The individual differences and individual variability of FD correlates closely with these branching characteristics. Therefore, these parameters should be taken into consideration for calculation of the normal values of the FD of skeletonized MR images of the cerebellum.

We compared the FD values of cerebellum obtained in the present study with the FD values received during studies conducted by other researchers to uncover possible differences in FD values and to identify possible factors that may determine these differences. In accessible literature, we found the group of

research works which involved fractal analysis of the MR images of the cerebellum [10–13]. Two-dimensional (2D) [10,11] and three-dimensional (3D) [12,13] fractal dimensions were assessed in those studies using different modifications of fractal analysis and the values of the FD obtained in those studies differed from the data obtained in our present study.

The 2D fractal dimension values of the two-dimensional MR-images of the cerebellum were calculated using the box counting method [10,11]. The MRI scans of 16 conditionally healthy persons were investigated. The mean FD value of the white matter was 1.49 ± 0.06. The study showed that patients with Chiari malformation type I had significantly reduced FD values of cerebellar white matter [10,11]. This FD value was close to the FD(S) value, obtained in the present study, because skeletonizing procedure revealed the main branches of the cerebellar white matter. Thus, the FD(S) characterized the structure of the cerebellar white matter. Meanwhile, our fractal dimension of the cerebellar tissue as a whole, FD (100), exceeded the values of the fractal dimension obtained in those studies [10,11].

The values of the 3D fractal dimension of the cerebellar MR images were determined using the box counting and pixel dilation methods in the other studies [12,13]. Usually, the values of the 3D fractal dimension vary from 2 to 3 and theoretically always exceed the two-dimensional FD values, which vary from 1 to 2. The values of the three-dimensional fractal dimension of the skeletonized digital images of the cerebellum were estimated in the work of Liu J.Z. *et al.*[12]. The mean value of 3D fractal dimension of the white matter was 2.26 ± 0.05 and the mean value of 3D fractal dimension of the gray matter was 2.49 ± 0.04. The pixel dilation method was used for fractal analysis. The skeletonizing procedure was used only as an image pre-processing method. In the other study [13], the values of 3D fractal dimension of the cerebellum were determined using the box counting method. The T1-weighted MR images were used in the study. The mean value of 3D fractal dimension of the white matter was 2.2746 ± 0.0446 and the mean value of 3D fractal dimension of the gray matter was 2.5267 ± 0.0228. The results of that study showed that patients with multiple system atrophy of the cerebellar type presented significantly lower FD values compared to the control group [13].

Thus, the values of the fractal dimension estimated by different modifications of the fractal analysis and on different types of MR images, with different algorithms of image segmentation, may be quite different. Therefore, to determine the normal values of the FD, it is important to take into account the peculiarities of the research methodology, as well as factors influencing the fractal properties of the object, since the fractal dimension is not a completely independent quantity.

The main limitations of our study are the small sample size (30 cerebellar MR images) and the small age range (18-30 years of age). Further studies with larger sample sizes and greater age range will be needed to determine the age peculiarities and the age changes of cerebellar fractal dimensions and quantitative parameters of the cerebellar white matter.

CONCLUSIONS

The present study demonstrates the main branching characteristics of the human cerebellar white matter by the use of quantitative morphological assessment and fractal dimension analysis. It can be concluded that the FD values of human cerebella depend on the branching parameters of the white matter on the cerebellar skeletonized MR images. The combined use of quantitative morphologic assessment and fractal analysis of the skeletonized MR images of the human cerebellum allows the evaluation of the spatial structural complexity and the degree of branching of the cerebellar white matter, and may be used to diagnose various diseases of the cerebellum. The obtained data can be employed as quantitative criteria in the estimation of the morphofunctional state of the human cerebellum using magnetic resonance imaging modality.

ABBREVIATIONS

2D: two-dimensional

3D: three-dimensional

FD(100): fractal dimension of non-skeletonized images

FD(S): fractal dimension of skeletonized images

FD: fractal dimension

MR images: magnetic resonance images

MRI: magnetic resonance imaging

ACKNOWLEDGMENTS

None

AUTHOR'S CONTRIBUTIONS

All authors equally contributed to this work. All authors read and approved the final manuscript.

FUNDING

None

AVAILABILITY OF DATA AND MATERIALS

Data and materials used and/or analyzed during the current study are available from the corresponding author on reasonable request.

ETHICS APPROVAL AND CONSENT TO PARTICIPATE

The study was conducted in compliance with the basic bioethical provisions of the Council of Europe Convention on Human Rights and Biomedicine (March 4, 1997), the Helsinki Declaration of the World Medical Association on the ethical principles of scientific medical research with human participation (1964-2008), and the order of Ministry of Health of Ukraine No. 690 dated Sept. 23, 2009. The conclusion of the Commission on Ethics and Bioethics of Kharkiv National Medical University confirmed that the study was conducted in compliance with human rights, in accordance with the current legislation in Ukraine, met international ethical requirements and did not violate ethical standards in science and standards of biomedical research (minutes of the meeting of the commission on ethics and bioethics of KhNMU No. 10 of Nov. 7, 2018). All participants provided written informed consent.

CONSENT FOR PUBLICATION

Not applicable.

COMPETING INTERESTS

The authors declare that they have no competing interests.

REFERENCES

1. Hasan KM, Mwangi B, Keser Z, Riascos R, Sargsyan AE, Kramer LA. Brain Quantitative MRI Metrics in Astronauts as a Unique Professional Group. J Neuroimaging. 2018;28(3):256–68. PMID: 29460455. Available from: 10.1111/jon.12501.
2. Yousaf T, Dervenoulas G, Politis M. Advances in MRI Methodology. Int Rev Neurobiol. 2018;141:31–76. PMID: 30314602. Available from: 10.1016/bs.irn.2018.08.008.
3. Zhou Y. Quantitative PET/MRI Evaluation and Application in Dementia. Jacobs J Med Diagn Med Imaging. 2016;1(1):5. PMID: 28008425.
4. Diedrichsen J, Balsters JH, Flavell J, Cussans E, Ramnani N. A probabilistic MR atlas of the human cerebellum. Neuroimage. 2009;46(1):39–46. PMID: 19457380. Available from: 10.1016/j.neuroimage.2009.01.045.
5. Park MT, Pipitone J, Baer LH, Winterburn JL, Shah Y, Chavez S. Derivation of high-resolution MRI atlases of the human cerebellum at 3T and segmentation using multiple automatically generated templates. Neuroimage. 2014;95:217–31. PMID: 24657354. Available from: 10.1016/j.neuroimage.2014.03.037.
6. Ieva AD, Grizzi F, Jelinek H, Pellionisz AJ, Losa GA. Fractals in the Neurosciences, Part I: General Principles and Basic Neurosciences. Neuroscientist. 2014;20(4):403–17. PMID: 24362815. Available from: 10.1177/1073858413513927.
7. Ieva AD, Esteban FJ, Grizzi F, Klonowski W, Martín-Landrove M. Fractals in the neurosciences, Part II: clinical applications and future perspectives. Neuroscientist. 2015;21(1):30–43. PMID: 24362814. Available from: 10.1177/1073858413513928.
8. Milosević NT, Ristanović D. Fractality of dendritic arborization of spinal cord neurons. Neurosci Lett. 2006;396(3):172–6. PMID: 16364544. Available from: 10.1016/j.neulet.2005.11.031.
9. Zaletel I, Ristanović D, Stefanović BD, Puškaš N. Modified Richardson's method versus the box-counting method in neuroscience. J Neurosci Methods. 2015;242:93–6. PMID: 25601478. Available from: 10.1016/j.jneumeth.2015.01.013.
10. Akar E, Kara S, Akdemir H, Kış A. Fractal analysis of MR images in patients with Chiari malformation: the importance of preprocessing. Biomed Signal Process Control. 2017;31:63–70. Available from: 10.1016/j.bspc.2016.07.
11. Akar E, Kara S, Akdemir H, Kış A. Fractal dimension analysis of cerebellum in Chiari Malformation type I. Comput Biol Med. 2015;64:179–86. PMID: 26189156. Available from: 10.1016/j.compbiomed.2015.06.024.
12. Liu JZ, Zhang LD, Yue GH. Fractal dimension in human cerebellum measured by magnetic resonance imaging. Biophys J. 2003;85(6):4041–6. PMID: 14645092. Available from: 10.1016/S0006-3495(03)74817-6.
13. Wu YT, Shyu KK, Jao CW, Wang ZY, Soong BW, Wu HM. Fractal dimension analysis for quantifying cerebellar morphological change of multiple system atrophy of the cerebellar type (MSA-C). Neuroimage. 2010;49(1):539–51. PMID: 19635573. Available from: 10.1016/j.neuroimage.2009.07.042.
14. Collantoni E, Madan CR, Meneguzzo P, Chiappini I, Tenconi E, Manara R, et al. Cortical Complexity in Anorexia Nervosa: A Fractal Dimension Analysis. Journal of Clinical Medicine. 2020;9(3):833. Available from: 10.3390/jcm9030833.
15. Fernández E, Jelinek HF. Use of fractal theory in neuroscience: methods, advantages, and potential problems. Methods. 2001;24(4):309–21. PMID: 11465996. Available from: 10.1006/meth.2001.1201.
16. Grizzi F, Castello A, Qehajaj D, Russo C, Lopci E. The Complexity and Fractal Geometry of Nuclear Medicine Images. Mol Imaging Biol. 2019;21(3):401–9. PMID: 30003453. Available from: 10.1007/s11307-018-1236-5.
17. Krohn S, Froeling M, Leemans A, Ostwald D, Villoslada P, Finke C. Evaluation of the 3D fractal dimension as a marker of structural brain complexity in multiple-acquisition MRI. Hum Brain Mapp. 2019;40(11):3299–320. PMID: 31090254. Available from: 10.1002/hbm.24599.
18. Michallek F, Dewey M. Fractal analysis in radiological and nuclear medicine perfusion imaging: a systematic review. Eur Radiol. 2014;24(1):60–9. PMID: 23974703. Available from: 10.1007/s00330-013-2977-9.
19. Smitha KA, Gupta AK, Jayasree RS. Fractal analysis: fractal dimension and lacunarity from MR images for differentiating the grades of glioma. Phys Med Biol. 2015;60(17):6937–47. PMID: 26305773. Available from: 10.1088/0031-9155/60/17/6937.
20. Squarcina L, Luca AD, Bellani M, Brambilla P, Turkheimer FE, Bertoldo A. Fractal analysis of MRI data for the characterization of patients with schizophrenia and bipolar disorder. Phys Med Biol. 2015;60(4):1697–716. PMID: 25633275. Available from: 10.1088/0031-9155/60/4/1697.
21. Zhang L, Butler AJ, Sun CK, Sahgal V, Wittenberg GF, Yue GH. Fractal dimension assessment of brain white matter structural complexity post stroke in relation to upper-extremity motor function. Brain Res. 2008;1228:229–40. PMID: 18590710. Available from: 10.1016/j.brainres.2008.06.008.
22. Zhao G, Denisova K, Sehatpour P, Long J, Gui W, Qiao J, et al. Fractal Dimension Analysis of Subcortical Gray Matter Structures in Schizophrenia. PLoS One. 2016;11(5):e0155415. Available from: 10.1371/journal.pone.0155415.
23. Milosević NT, Ristanović D, Stanković JB. Fractal analysis of the laminar organization of spinal cord neurons. J Neurosci

Methods. 2005;146(2):198–204. PMID: 16054510. Available from: 10.1016/j.jneumeth.2005.02.009.

24. Puškaš N, Zaletel I, Stefanović BD, Ristanović D. Fractal dimension of apical dendritic arborization differs in the superficial and the deep pyramidal neurons of the rat cerebral neocortex. Neurosci Lett. 2015;589:88–91. PMID: 25603473. Available from: 10.1016/j.neulet.2015.01.044.

25. Ristanović D, Nedeljkov V, Stefanović BD, Milosević NT, Grgurević M, Stulić V. Fractal and nonfractal analysis of cell images: comparison and application to neuronal dendritic arborization. Biol Cybern. 2002;87(4):278–88. PMID: 12386743. Available from: 10.1007/s00422-002-0342-1.

26. Ristanović D, Stefanović BD, Puškaš N. Fractal analysis of dendrite morphology of rotated neuronal pictures: the modified box counting method. Riv Biol. 2014;107(1-2):109–21. PMID: 25936217.

27. Ieva AD. Fractal analysis of microvascular networks in malignant brain tumors. Clin Neuropathol. 2012;31(5):342–51. PMID: 22939175. Available from: 10.5414/np300485.

28. Lorthois S, Cassot F. Fractal analysis of vascular networks: insights from morphogenesis. J Theor Biol. 2010;262(4):614–33. PMID: 19913557. Available from: 10.1016/j.jtbi.2009.10.037.

29. Wang R, Li P, Pan Q, Li JK, Kuebler WM, Pries AR. Investigation into the diversity in the fractal dimensions of arterioles and venules in a microvascular network - A quantitative analysis. Microvasc Res. 2019;125:103882. PMID: 31075242. Available from: 10.1016/j.mvr.2019.103882.

30. McCreary CR, Beaudin AE, Subotic A, Zwiers AM, Alvarez A, Charlton A. Cross-sectional and longitudinal differences in peak skeletonized white matter mean diffusivity in cerebral amyloid angiopathy. Neuroimage Clin. 2020;27:102280. PMID: 32521475. Available from: 10.1016/j.nicl.2020.102280.

31. Bai X, Ye L, Zhu J, Zhu L, Komura T. Skeleton Filter: A Self-Symmetric Filter for Skeletonization in Noisy Text Images; 2019. Available from: 10.1109/TIP.2019.2944560.

32. Greenblum A, Sznitman R, Fua P, Arratia PE, Oren M, Podbilewicz B. Dendritic tree extraction from noisy maximum intensity projection images in C. elegans. Biomed Eng Online. 2014;13(1):74. PMID: 25012210. Available from: 10.1186/1475-925X-13-74.

33. Orlowski D, Bjarkam CR. A simple reproducible and time saving method of semi-automatic dendrite spine density estimation compared to manual spine counting. J Neurosci Methods. 2012;208(2):128–33. PMID: 22595026. Available from: 10.1016/j.jneumeth.2012.05.009.

34. Prodanov D, Verstreken K. Automated Segmentation and Morphometry of Cell and Tissue Structures.; 2012. Available from: 10.5772/36729.